STANDOFF RAMAN SPECTROSCOPY SYSTEM FOR DETECTION OF EXPLOSIVES, CHEMICAL WARFARE AGENTS SIMULANTS AND TOXIC INDUSTRIAL COMPOUNDS

By

William Ortiz Rivera

A thesis submitted in partial fulfillment of the requirements for the degree of

MASTER OF SCIENCE
In
Chemistry

UNIVERSITY OF PUERTO RICO
MAYAGUEZ CAMPUS
2008

Approved by:

_____   _____
Samuel P. Hernández Rivera, Ph.D.   Date
President, Graduate Committee

_____   _____
Mayra E. Cádiz García, Ph.D.   Date
Member, Graduate Committee

_____   _____
Nairmen Mina Camilde, Ph.D.   Date
Member, Graduate Committee

_____   _____
Ivan Baiges Valentin, Ph.D.   Date
Representative of Graduate studies

_____   _____
Francis Patron, Ph.D.   Date
Chairperson of the Department

ABSTRACT

In this work a remote Raman system has been designed, assembled and tested for detecting explosives, Toxic Industrial Compounds (TIC) and Chemical Warfare Agents Simulants (CWAS) at laboratory scale up to 7 m target-telescope distance. The prototype system consists of a Renishaw Raman Microspectrometer, model RM2000, equipped with a charge-coupled device (CCD) detector, a telescope, a fiber optic assembly and a single wavelength/frequency laser source (514/488 nm and 532 nm). The telescope was coupled to the Raman microscope using an optical fiber and filters for rejection of laser radiation and Rayleigh scattering. Two convex lenses collimate the light from the telescope output, which is directed into the fiber optic from which the focusing objective was removed. The output of the fiber was directly coupled to the Raman system by a 5x objective. To test the standoff sensing system, the VIS Raman Telescope was used in detection of secondary explosives: 2,4,6-trinitrotoluene (TNT), 2,4-dinitrotoluene (2,4-DNT), hexahydro-1,3,5-trinitro-1,3,5-triazine (RDX), triacetone triperoxide (TATP) and plastic explosive C4, with detection limits below 10 mg. The TICs used were benzene, toluene, xylenes, chloroform, CCl_4 and CS_2. Other compounds studied were Chemical Warfare Agents Simulants dimethylmethyl phosphonate (DMMP), 2-chloroethyl ethyl sulfide (2-CEES). Solid samples (explosives) were deposited on stainless steel plates and liquid samples were transferred into 5 mL glass vials. Both types of samples were placed at a distance of 7 m from the telescope. Raman spectra of compounds were acquired in the Raman shift range of 100-3200 cm^{-1} using laser powers varying from 50 mW to 1 W and integration times of 1 to 30 s.

RESUMEN

En este trabajo se diseñó un sistema de detección remota Raman, el cual se utilizó en la detección de explosivos, simulantes de agentes de guerra químicos y compuestos tóxicos industriales a una distancia del telescopio-muestra de 7 m. El diseño consiste de un microespectrómetro Raman Renishaw modelo RM2000 equipado con un detector CCD, un telescopio, una fibra óptica y una fuente de láser (514/488 nm o 532 nm). El telescopio se acopló al microscopio Raman por medio de una fibra óptica. Dos lentes convexos coliman la luz proveniente de la salida del telescopio, la cual converge directamente sobre la fibra óptica, la salida de la fibra se acopló al sistema Raman mediante un objetivo de 5x. El sistema de detección remota se verificó utilizando explosivos secundarios: TNT, 2,4-DNT, RDX, TATP y el explosivo plástico C4, con limites de detección por debajo de 10 mg. Los compuestos tóxicos industriales empleados fueron benceno, tolueno, xylenos, cloroformo, CCl_4 y CS_2. Otros compuestos estudiados fueron los simulantes de agentes de guerra químicos: dimetilmetilfosfonato (DMMP) y 2-cloroetiletilsulfuro (2-CEES). Las muestras solidas se depositaron sobre láminas de acero inoxidable y las muestras líquidas se transfirieron a frascos de 5 mL. Ambos tipos de muestras se colocaron a una distancia de 7 m del telescopio. Los espectros de los compuestos se adquirieron en el rango de dispersión Raman de 100-3200 cm^{-1} utilizando potencias del láser de 50 mW a 1 W y tiempos de integración de 1 a 30 s.

To my family

ACKNOWLEDGEMENTS

I would like to express my most sincere appreciation to all the people that in one way or another have contributed positively in the completion of this research.

Sincerely I thank the Almighty for giving me the wisdom, patience and above all perseverance to be able to overcome all obstacles and challenges in the wonderful world of science.

I immensely thank my advisor Dr. Samuel P. Hernández for giving me the opportunity to do research under his guidance and supervision in the Center for Chemical Sensors Development. I also wish to share this acknowledgement with my partners and peers from Dr. Hernández's laboratory, especially Leonardo Pacheco for his valuable intellectual contribution to this research.

To my friends: Omar, Wilman, Pedro, Oliva, Luis Fernando, Sandra, Bibiana, Hilsamar, Jorge and Jenifier for all the pleasant and fun moments we shared in my stay in graduate study.

TABLE OF CONTENTS

LIST OF TABLES

LIST OF FIGURES

1. INTRODUCTION

During recent years, the world has suffered many terrorist attacks by use of explosives and chemical warfare agents, such as the attack in London on July 7, 2005 (also called the 7/7 bombings), where several explosions in a bus and four subway stations occurred almost simultaneously during the rush hours of the morning. These events completely affected the entire underground network and buses, casting shadows on the joy of Londoners, who had been recently selected as hosts for the 2012 Olympic Games. On the other hand, another fatal attack occurred in New York, also called 9/11 where an Al Qaeda related terrorist group highjacked several commercial aircrafts and destined them to crash into the World Trace Center buildings, where many people lost their lives. These and other terrible events have motivated many countries to focus their research toward the detection of explosives, hazardous liquids, and chemical agents that can be employed by terrorist organizations as threats against troops and/or civilians. The anticipation of future attacks requires a wide array of detection systems for potential deployment scenarios.[1, 2]

An explosive is described as a metastable agent before detonation. Actual detonation is characterized by extremely rapid reaction rates, measured in milliseconds. Products of this detonation are gasses, heat and high pressures. Explosives can be classified by their performance and uses. Primary explosives also known as low explosives undergo very rapid transition from burning to detonation. These are capable of transmitting the detonation to less sensitive explosives. Detonation can occur by heat or shock. Examples of primary explosives are mercury fulminate and lead azide. Secondary explosives, also

known as high explosives, cannot be detonated readily by heat or shock and they are less sensitive than primary explosives, so they need the later to detonate. Examples of secondary explosives are 2,4-dinitrotoluene (DNT), 2,4,6-trinitrotoluene (TNT), triacetone triperoxide (TATP) and hexahydro-1,3,5-trinitro-1,3,5-triazine (RDX). TNT is one of the high explosives that has been used for military purposes since 1902.

Chemical Warfare Agents (CWA) most likely to be used as terrorist weapons, according to terrorism experts include nerve agents, blister agents, choking agents and blood agents. Nerve agents are a group of particularly toxic chemical warfare agents.[3, 4] They were developed just before and during World War II and are chemically related to organophosphorus insecticides. The principal compounds in this group are: Tabun (GA), Sarin (GB), Soman (GD), and methylphosphonothioic acid (VX). Characterization of hydrolysis and or degradation products of CWA has been documented to provide still another capability to detect possible attacks to water systems.[2, 3]

During the last few years, the topic of explosives detection has been an active research area. The need for security screening introduced a variety of schemes for detection of trace amounts of energetic materials.[5] Several techniques have been employed to detect and identify explosives, hazardous liquids and chemical warfare agents simulants including HPLC/MS, GC/MS, IMS, Infrared Spectroscopy, Raman Spectroscopy, among others. Vibrational spectroscopy has the advantage that provides chemical information besides detection capabilities. Raman spectroscopy is a non-destructive and non-invasive technique that requires little sample treatment and has the potential for remote sensing.

There is a need for more sensitive and selective remote detection techniques for explosives operating at ambient conditions, *in situ* and in real-time scale. Therefore, Standoff Raman spectroscopy (SRS) provides a method for identifying chemicals in a sample located meters from the excitation source. In fact, telescope based Raman spectroscopy detection methods have been reported for standoff detection of chemicals using both visible and UV laser excitation.[6-13] This distance can vary from a few centimeters, for monitoring chemicals in a manufacturing process, to tens of meters when examining potentially-dangerous samples such as explosives. SRS has been demonstrated and is used in several areas, including explosives detection, atmospheric analysis and detection of different organic and inorganic compounds.

1.1 OBJECTIVE

The objective of this work was to design and assemble a visible region Raman telescope and to demonstrate, at laboratory scale, the capability of Raman Spectroscopy as a tool in remote sensing technology. The standoff sensing system was tested for the detection of explosives (TNT, RDX, PETN, C4 and Semtex) and hazardous liquids (benzene, toluene, ethyl benzene, xylenes (BTEX)). Other compounds that were studied included Chemical Warfare Agents Simulants, such as dimethylmethyl phosphonate (DMMP), 2-chloroethyl ethyl sulfide (2-CEES) and di-isopropylmethyphosphonate (DIMP)). This objective was accomplished using a Raman Microspectrometer equipped with 488 and 514 nm excitation lines from a Coherent INNOVA 308 Ar^+. The spectroscopic system was coupled to a reflective optical telescope typically used in astronomy via optical fibers of 600 μm inner diameter.

2. PREVIOUS WORK

During the past few years, researchers have dedicated part of their time and efforts to study the detection of explosives, hazardous liquids, and chemical agents on many surfaces and into bottles. Recent work has led to development of methods to couple Raman system to light collecting systems, i.e., telescopes.

In 2003, Sharma et al. developed a version of a visible region, standoff Raman spectroscopic system, using Maksutov-Cassegrain telescope and a pulsed laser (20 Hz, 532 nm, Nd:YAG).[12] This system was capable of measuring the Raman spectra of benzene in liquid and vapor phase and minerals located at a distance of 4.5-10 m from the telescope. Sharma et al. in 2005 used a small portable Raman system for standoff detection and identification of various types of organic chemicals including benzene, toluene, ethyl benzene and xylenes (BTEX).[13] Both fiber optic (FO) coupled and a directly coupled telescope to an f/2.2 spectrograph were developed and tested. A frequency-doubled Nd:YAG pulsed laser (20 Hz, 532 nm, 35 mJ/pulse) were used as excitation source. The operational range of the FO coupled Raman system was tested to 66 m, and the directly coupled system was tested to a distance of 120 m. They also measured remote Raman spectra of two explosives: tri-aminotrinitrobenzene (TATB) and beta-HMX at 10 m standoff distance.

Carter et al. (2005) designed and demonstrated a standoff Raman system for detecting high explosive materials at distances up to 50 meters in ambient light conditions.[15] In the system, light was collected using an 8-in. Schmidt–Cassegrain telescope fiber-coupled to

an f/1.8 spectrograph with a gated intensified charge-coupled device (ICCD) detector. A frequency-doubled Nd:YAG (532 nm) pulsed (10 Hz) laser was used as the excitation source for measuring remote spectra of samples containing up to 8% explosive materials. The explosives RDX, TNT, and PETN as well as nitrate- and chlorate-containing materials were used to evaluate the performance of the system with samples placed at distances of 27 and 50 meters. Laser power studies were performed to determine the effects of laser heating and photodegradation on the samples.

In 2006 Aunupam et al. obtained Raman spectra of common minerals and organic (benzene, cyclohexane, 2-propanol, naphthalene, etc.) compounds from a small portable instrument at a distance of 10 m in a well illuminated laboratory with a single 532 nm laser pulse of energy of 35 mJ/pulse. [14]

3. THEORY OVERVIEW

3.1 Raman spectroscopy

Raman spectroscopy is a high resolution photonic technique that provides in a few seconds to minutes spectroscopic information that can be used to convey chemical and structural information about any organic and inorganic compounds. The Raman effect was originally observed in 1928 (Figure 1) by the physicist Chandrasakhar V. Raman. Sir C.V. Raman first observed the phenomenon using sunlight and was awarded the Nobel Prize in Physics for this discovery in 1930.[17]

The Raman event occurs when a monochromatic light of frequency v_o encounters a sample (gas, solid or liquid). When analyzing the light scattered by the sample, it is found that most of the scattered light presents the same frequency as the incident light (elastically scattered radiation). The light that keeps the same frequency v_o that the incident light is known as elastic or Rayleigh scattering and provides no information on the composition of the sample. A small fraction of the emerging light photons shows frequency shifts resulting from the interaction of light with matter (inelastically scattered radiation). Scattered light that presents different frequencies to that of the incident radiation is known as Raman scattering. The new frequencies $v_o + v_R$ and $v_o - v_R$ are Raman frequencies, which are characteristic of the nature and physical state of the sample and independent of the incident radiation.

Variations in the observed frequency in Raman scattering phenomenon, are equivalent to variations in energies. Ions and atoms chemically bonded to form molecules and crystalline networks are subjected to constant vibrational and rotational movements; these

15

oscillations are observed at certain frequencies based on the masses of particles involved and the dynamic behavior of the bond that exist. Each of these vibrational and rotational movements of the molecule and correspond to a certain value of molecular energy.

When the photon beam incident light, with energy ($h\nu_o$) much greater than the difference in energy between two vibrational (or rotational) levels of the molecule collides with the molecule, most of the photons pass by without interacting with the molecular system; but a small fraction are scattered (of the order of 1 scattered photon per 10^6 incident photons). This scattering can be interpreted as the following process: the incident photon leads the molecule temporarily to a higher level of energy vibrational or rotational (virtual state) which is not an allowed or stationary state, which quickly decays to an allowed energy level emitting a photon.

If scattered photon is the result of the photon-molecule interaction, its frequency differs of the incident frequency, this collision is termed inelastic. This means that there is a transfer of energy between the photon and the molecule, in this case two phenomena may occur: If the scattered photon has lower frequency than the incident one, there is a transfer of energy from photon to the molecule that after moving into a forbidden energy state, and returns to its allowed initial energy state, the photon is scattered with frequency $\nu_o - \nu_R$ and Stokes Raman dispersion occurs. Another possible phenomenon occurs if the scattered photon has a higher frequency than the incident, there is a transfer of energy from the molecule to the photon; this means that initially before the collision occurred the molecule was not in its lowest vibrational state, but one of higher energy. After the collision takes place, the photon is scattered with a frequency $\nu_o + \nu_R$ and Raman anti-Stokes scattering occurs.

At room temperature, according to the Maxwell-Boltzmann law of distribution of energy, 99% of the molecules are in the lowest possible vibrational state (ground vibrational state). Therefore, the probability of Raman Stokes scattering occurrence are greater than the Raman anti Stokes scattering. These processes are illustrated in Figure 1.
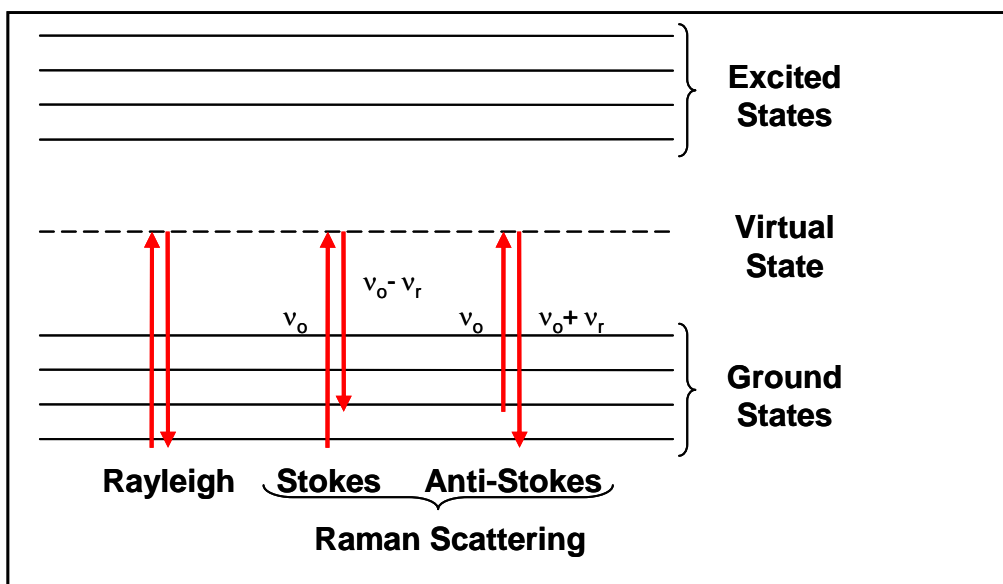

Figure 1. Energy Diagram for Raman Scattering.

4. MATERIALS AND METHODS

4.1 Reagents

The reagents that were used in this investigation were:

1. High explosives (HE), precursors and formulations: 2,4,6-trinitrotoluene (TNT, 99% Chem Service, West Chester, PA); hexahydro-1,3,5-trinitro-1,3,5-triazine (RDX, 99%, Chem Service); pentaerythritol tetranitrate (PETN), C4, Semtex-H; acetone (CH_3COCH_3, 98% w/w, Aldrich-Sigma Chemical Co., Milwaukee, WI), hydrogen peroxide (H_2O_2 50% in water, Aldrich-Sigma).

2. Toxic Industrial Compounds (TICs): methyl ether (CH_3OCH_3, Aldrich-Sigma); ethylbenzene, certified Fisher Scientific, International, (Cat # O2751-1, > 99%), toluene ACS certified, Fisher Cat. # AC42455-5000 (>99%), (o-m-p) xylenes, certified Fisher Scientific International, (Cat # O5078-1, >99%).

3. Chemical Warfare Agents Simulants (CWAS): dimethylmethyl phosphonate (DMMP, Fisher Scientific International, Chicago, IL); diisopropyl methylphosphonate (DIMP, Alfa Aesar, Ward Hill, MA), 2-chloroethyl ethyl sulfide (2-CEES, Sigma Aldrich Chemical Company, St. Louis, MO).

4.2 Sample preparation

All liquid reagents were deposited in glass vials, and solids reagents were deposited on the stainless steel slides.

4.3 Raman Instrumentation

Renishaw Raman Microspectrometer RM2000 system was employed for the vibrational spectroscopy measurements. The 514.5 and 488 laser lines of a Coherent INNOVA 308 argon ion laser and the 532 nm of a Coherent VERDI, 6 watts maximum power, solid state diode laser system were employed as excitation sources. Raman spectra of samples were collected in the Raman Shift range of 200-3600 cm^{-1}. Integration time from 1 to 30 seconds were used.

4.4   Optical Fiber cable

Premium Grade Xtreme XSR solarization-resistant Optical Fiber Assemblies were obtained from Ocean Optics, Inc. In particular, reflection/backscattering fiber optics probes operating in a wavelength range of 180-900 nm of 600 μm in diameter model # AL 1217 were used to interface the telescope to the Raman Microspectrometer

4.5   Telescope

A Meade ETX-125AT 5.0"/125mm Maksutov-Cassegrain reflective telescope (1900 mm; f/15) with motorized guidance system (Altazimuth Mount, Autostar computerized controller), 26 mm (73x) 1.25" eyepiece, 8x25 finderscope was used as light collector. The system was equipped with a tripod and a bench stand to allow for various applications.

5   RESULTS AND DISCUSSION

5.1   Raman telescope design

 The experimental setup for the prototype standoff Raman spectroscopy based system is schematically shown in Fig. 2. The prototype system consists of a Renishaw Raman Microspectrometer, model RM2000, equipped with an charge-coupled device (CCD) detector and the appropriate filters for rejection of satellite plasma lines (laser line filters) and laser radiation to block Rayleigh scattered light (notch filters), a telescope, a fiber optic assembly, and a single line/frequency laser system operating at 514/488nm (argon ion) and 532 nm (frequency doubled Nd:YAG solid state diode).
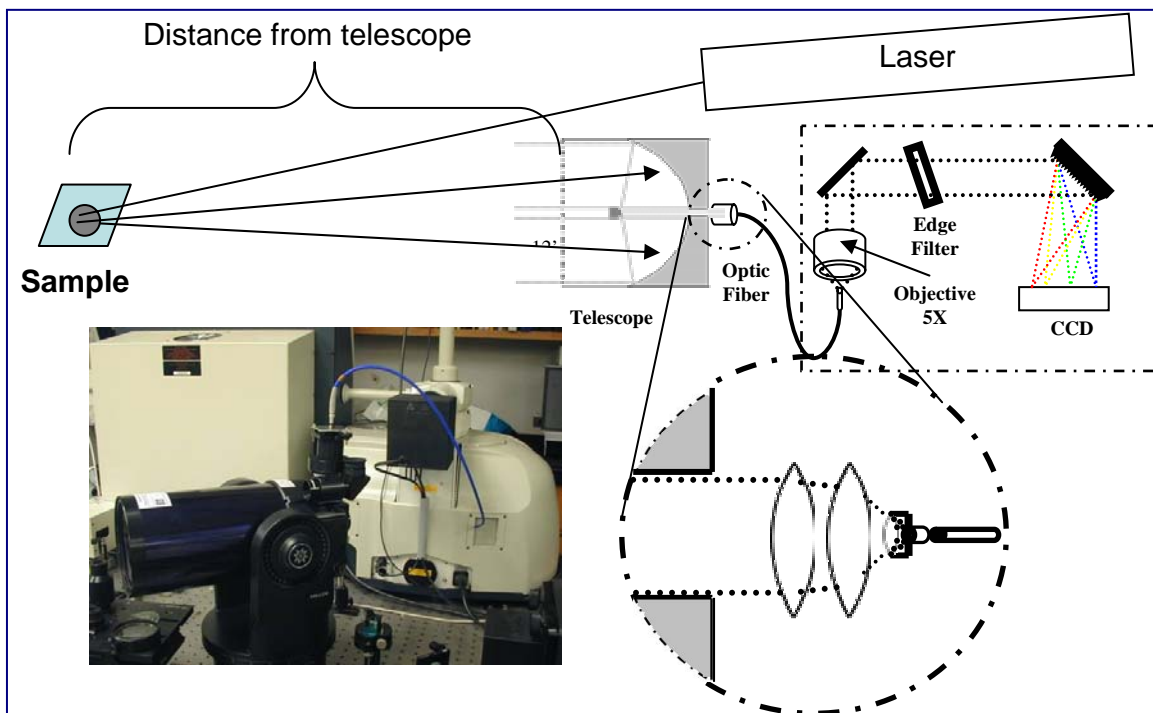

Figure 2. Design of standoff VIS Raman Telescope.

The telescope (MEADE ETX-125, Maksutov-Cassegrain design, 125 mm clear aperture, 1900 mm focal length, f/15) was coupled to the Raman microscope with an optical fiber (non-imaging, 600 μ diameter, model AL 1217, Ocean Optics, Inc.). Two lenses collimate the light from the telescope output, which is directed into the fiber optic from which the focusing objective was removed. The output of the fiber optic assembly was directly coupled to the Raman system by 5x objective. Neat liquid samples were placed into 5 mL glass vials and placed about 7-10 meters from telescope. Solid samples were smeared onto stainless steel plates under controlled conditions. Spectra of all compounds were measured in the Raman Shift range of 100-3200 cm^{-1} at laser powers from 50 mW to 1 W and integration times of 1 – 30 s.

5.2   Remote Raman Spectra of HEs and Comparison with Normal Raman Spectra

Remote Raman spectrum of RDX in region 150-3200 cm^{-1} at a distance of 7 m from the telescope is shown in Fig. 3**.** This sample was detected using a laser excitation wavelength of 514 nm with 1W power and an acquisition time of ten seconds for recording the spectrum. Figure 4 shows a comparison between the normal (or spontaneous) Raman (NR) spectrum of the important nitroaromatic high explosive (HE). Figures 4, 6, 8 and 10 illustrate a comparison between the Raman spectra employing telescope and microscope. For the Raman telescope spectrum of TNT, an absence of bands around 3100 cm^{-1} and at low frequencies is observed. For DNT's Raman telescope spectrum, no spectral difference is found except for low frequencies. However, for the

situation of RDX an absence of bands in the fingerprint region around 1400-1600 cm^{-1} and low frequencies are observed as well. There is no evidence about this phenomena, possibly this situation is due to optical interferences and fluorescence, which is persistent in every spectrum except for TATP and more notable in RDX.
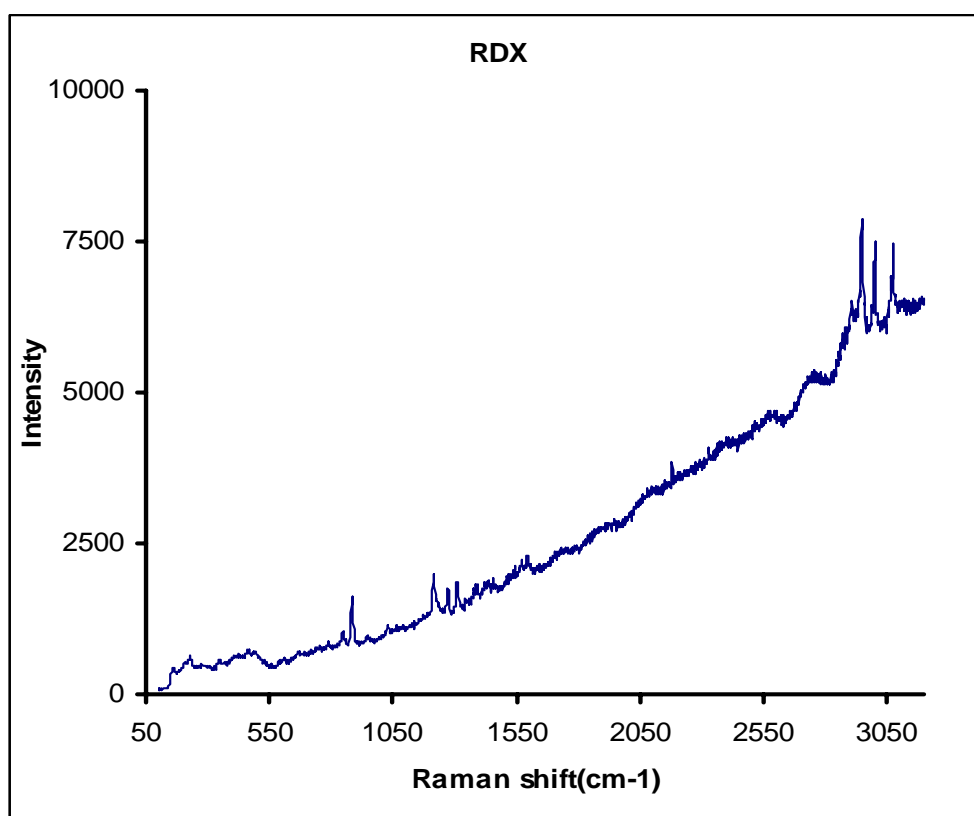
5.3   RDX

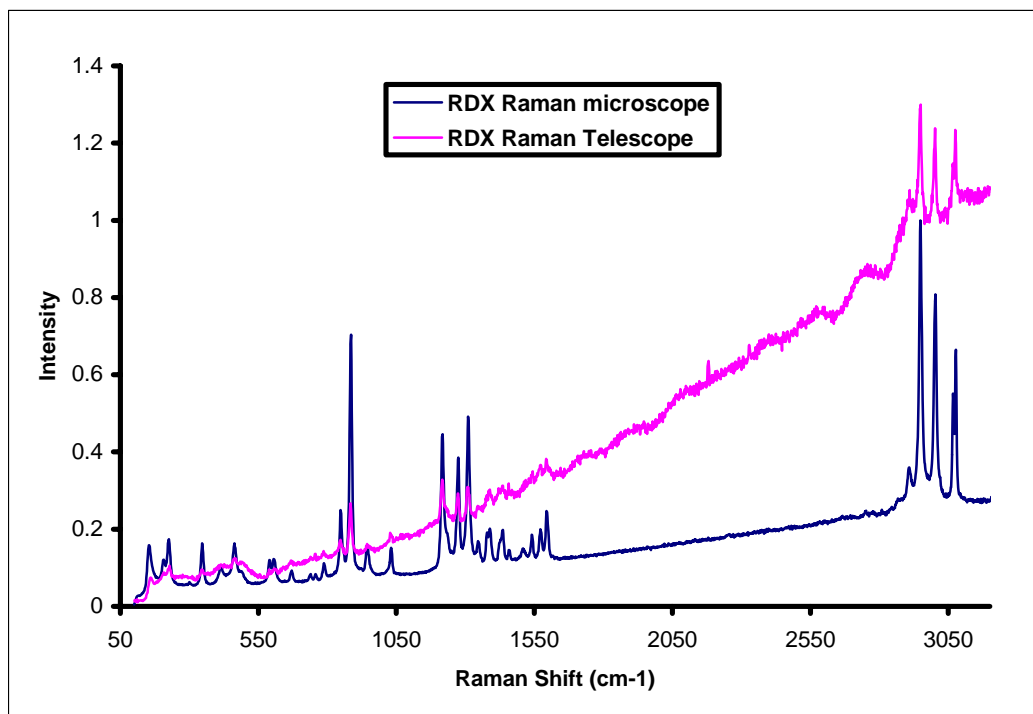**Figure 3 Remote Raman spectrum of RDX at 7 m, 488 nm, 1W and 10 s.**

22

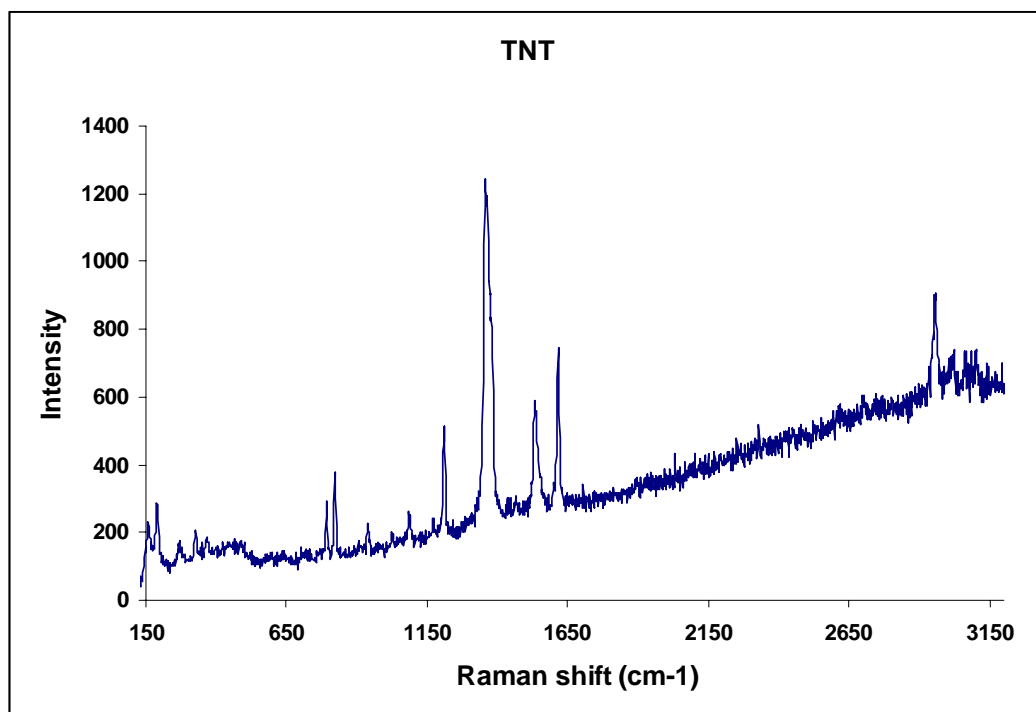**Figure 4 Raman telescope and Raman microscope spectra of RDX.**

5.4 TNT

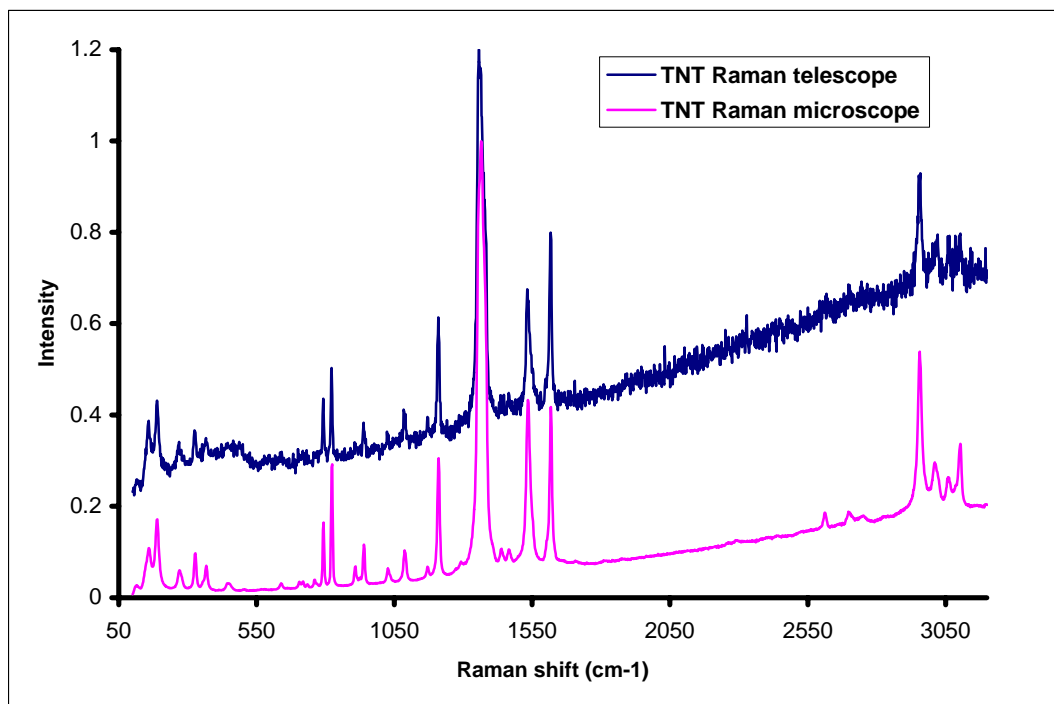**Figure 5 Remote Raman spectrum of TNT at 7 m, 514 nm, 1W and 10 sec.**

Figure 6 Comparison of Raman telescope and Raman microscope spectra of TNT.

The most important Raman signals that allowed the identification of TNT can be observed in table 1, Bands of the C-H region are observed at 3016 and 2955 cm^{-1}. These bands can be assigned to the aromatic C-H asymmetric stretching vibration and symmetric stretch, respectively, and belong to the alkyl CH_3 group. The principal peaks of high intensity are 1365 cm^{-1} (NO_2 symmetric stretching vibration), 1535 cm^{-1} (asymmetric NO_2 stretching), 1617 cm^{-1} (2,6-NO_2 asymmetric stretching vibration), 1210 cm-1 (C-H (ring) in plane bend, ring breathing). Very weak bands are observed at 822 cm^{-1} (nitro-group scissoring mode), and 792 cm^{-1} (C-CH_3 stretching, 2,4,6-NO_2 scissoring).

Table 1 Assignments of vibrational modes of TNT

Raman Frequencies cm $^{-1}$	Assignments
326	2,4,6 C-N in plane torsion
366	Methyl group deformation
792	C-CH3 stretching, 2,4,6 NO_2 scissors
822	2,4,6 NO_2 scissors
914	C-H (ring) out of plane bend
941	C-H (ring) out of plane bend
1091	C-H (ring) in plane bend
1175	Symmetric methyl C-C-H bending
1210	C-H (ring) in plane bend, ring breathing
1361	NO_2 symmetric, C-N stretching
1538	NO_2 Asymmetric stretching
1616	2,6 NO_2 Asymmetric stretching\
2956	C-H Asymmetric stretching
3016	Aromatic C-H stretching
3065	Aromatic C-H stretching

5.5 2,4-DNT

The remote Raman spectrum of 2,4-DNT (DNT), in the region 150-3200 cm^{-1},and at a distance of 7 m from the telescope is shown in Fig. 7. This sample was detected using a 514 nm laser beam with 1W and the acquisition time was 10 seconds for recording the spectrum. The reference micro Raman spectrum of DNT is compared to the RRS spectrum of DNT in Figure 6. According to the literature 2,4-DNT is characterized by six prominent bands in (table 2) the 750-1650 cm^{-1} region: a very strong peak at 1350 cm-1 (NO_2 symmetric stretching mode), two bands at 1514 cm^{-1} (asymmetric NO_2 stretching) and 1607 cm^{-1} (aromatic – NO_2 conjugation), one band at 1193 cm^{-1} (C-H in plane bend), a band at 1075 cm^{-1} (C-N-O bending mode) and one band at 792 cm^{-1} (C-H out-of-plane bend).
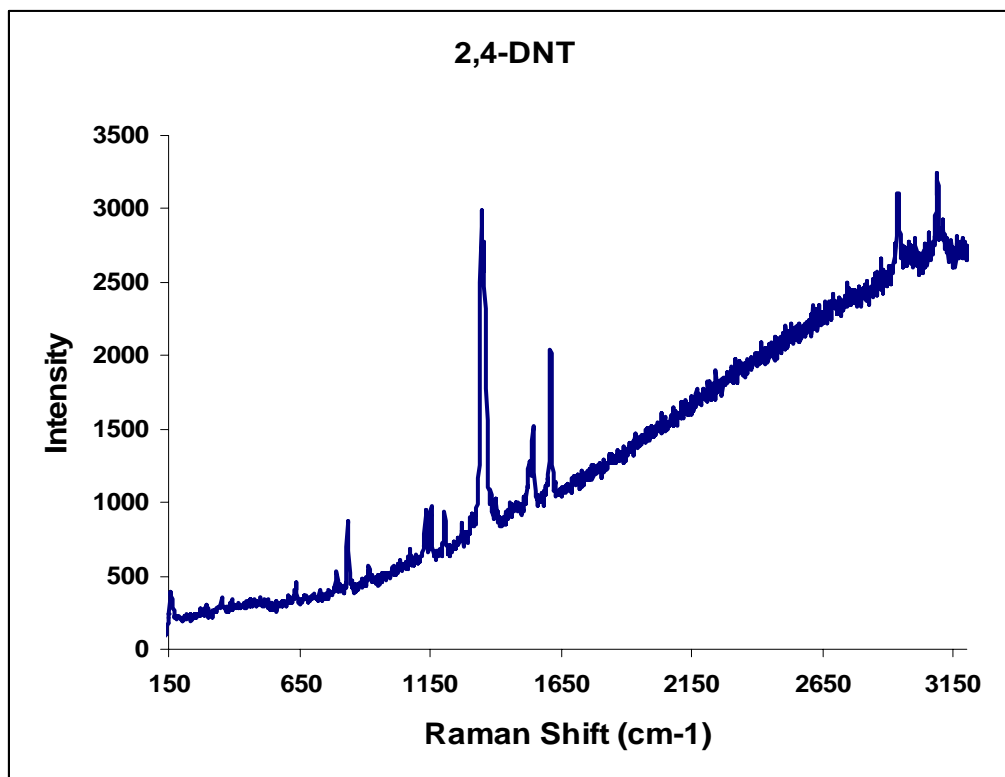

Figure 7 Remote Raman spectrum of 2,4-DNT at 7 m, 514 nm, 1W and 10 sec.
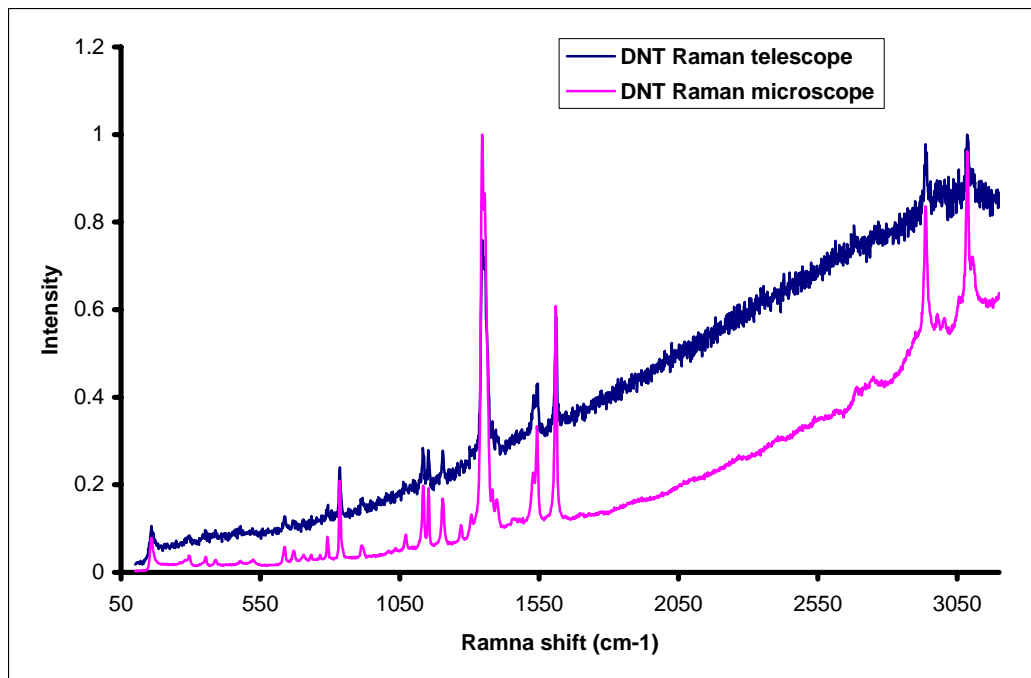
Figure 8 Comparison of Raman telescope and Raman microscope spectra of DNT.

The Raman Shift signal at 2940 cm^{-1} was assigned to the asymmetric C-H vibration of the CH$_3$ group. The peak found at 3100 cm^{-1} corresponds to the aromatic C-H stretching vibration.

Table 2 Assignments of vibrational modes of 2,4-DNT.

Raman cm^{-1}	Tentative Assignment 2,4-DNT
3100	aromatic C-H stretching vibration
3070	aromatic C-H stretching vibration
3021	aromatic C-H stretching vibration
2940	asymmetric C-H vibration of the CH_3 group
1607	aromatic- NO_2 conjugation
1514	asymmetric NO_2 stretching vibration
1445	C-C ring stretching
1350	symmetric NO_2 stretching vibration
1193	H-C-C in plane bend
1147	symmetric methyl H-C –H bend
1123	methyl H-C-H asymmetric bend
1075	C-N-Ó bend
1020	Out- of- plane bend of ring H
830	methyl rock
792	out-of- plane C-H and C-N bend
780	Nitro-group scissoring mode
717	C-N-Ó bend
560	ring deformation
100-500	Skeletal deformation of the aromatic ring

5.6   Remote Raman spectra of TATP

Figure 9 shows the remote Raman spectra of triacetone triperoxide. TATP is an explosive used by terrorist which has appeared as a weapon of mass destruction in the Middle East. It can be as or more powerful than some military analogs. TATP is one of the most sensitive explosives known, being extremely sensitive to impact, temperature change and friction. TATP can be easily prepared in a basement lab using commercially available starting materials obtained from, e.g., hardware stores, pharmacies, and stores selling cosmetics. TATP is a fairly easy explosive to prepare but highly unstable, as far as explosives manufacturing goes. All it requires is acetone, hydrogen peroxide and a strong acid such as hydrochloric or sulfuric acid.

The most important bands in the Raman spectrum of TATP appear around 860-1000 cm^{-1} corresponding to peroxide O-O stretching mode. The low-frequency bands near 550-600 cm^{-1} corresponding to the O-C-O bending motion.[21]
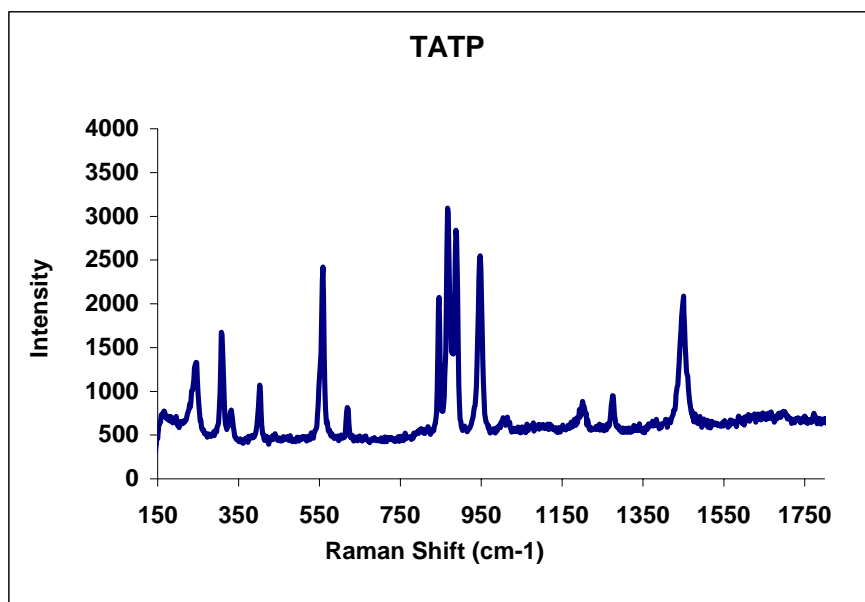

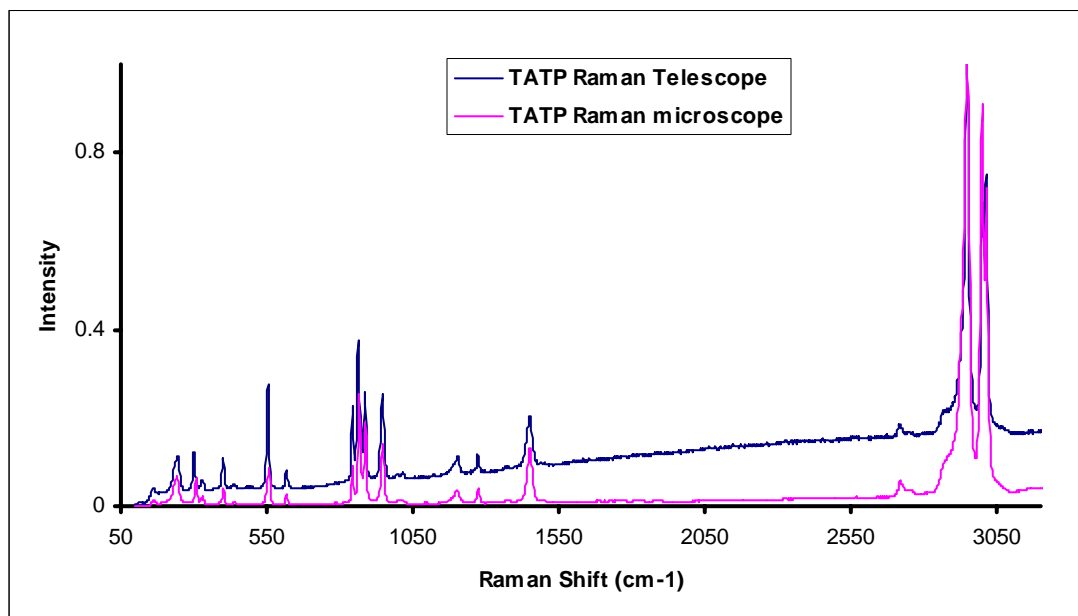**Figure 9 Remote Raman spectra of TATP.**

Figure 10 Comparison of Raman telescope and Raman microscope spectra of TATP.

5.7 Remote Raman spectra of plastic explosive C4

Cyclotrimethylenetrinitramine, $C_3H_6N_6O_6$ or RDX, which stands for Royal Demolition eXplosive is also known as cyclonite or hexogen. RDX is currently the most important military high explosive in the United States. It is second in strength to nitroglycerin among common high explosives substances. RDX can be mixed with plasticizers to make C-4, and combined with PETN to form the well known formulation Semtex. Semtex-H has an explosive composition of 50% RDX and PETN.

Remote Raman spectra of C4 (91 % RDX) in the Raman shift region 150-3200 cm^{-1} for a target to telescope distance of 7 m is shown in Fig. 11**.** This sample was detected using 488 nm laser beam with 1W and the acquisition time was 10 seconds for recording the spectrum.
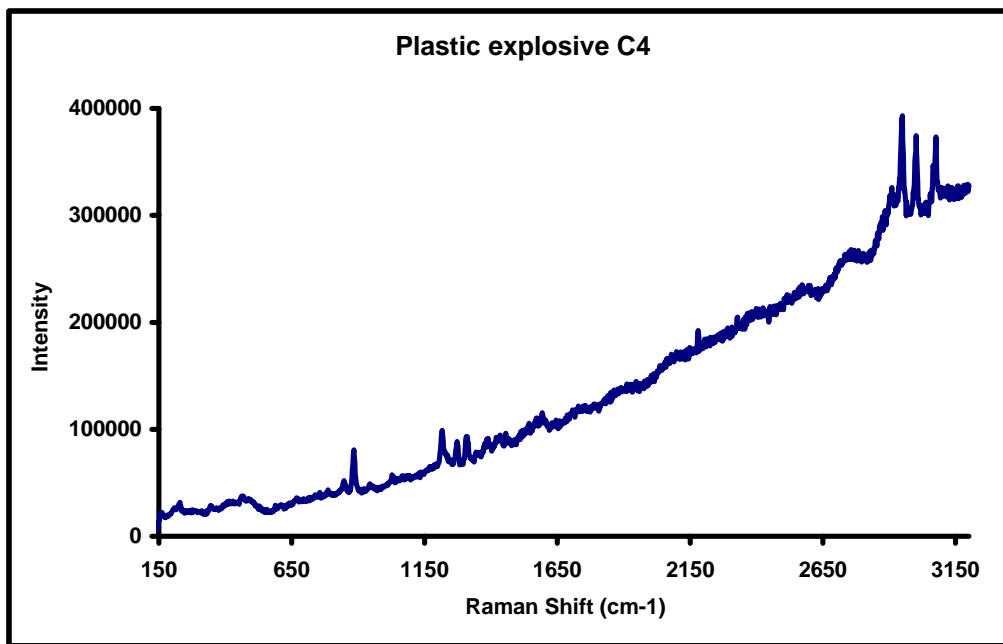
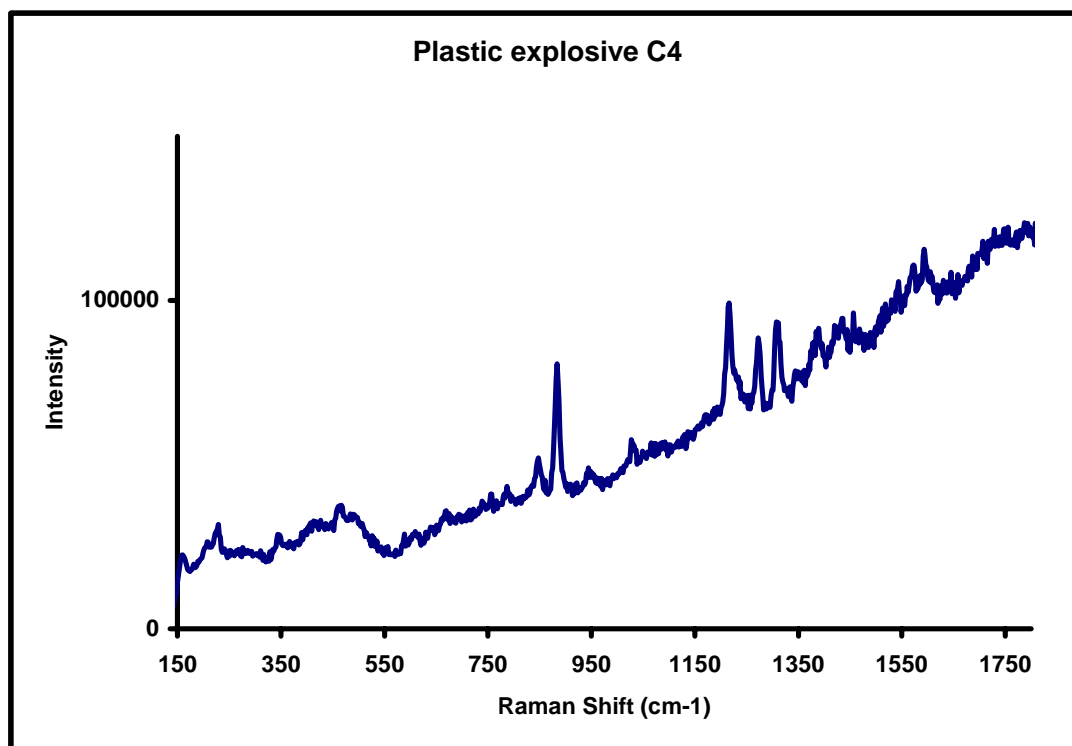**Figure 11 Remote Raman spectrum of C4 at 7 m, 488 nm, 1W and 10s.**

Figure 12 Remote Raman fingerprint region of C4.

Raman signals can be identified in the symmetric and asymmetric C-H bond-stretching region shown in Figure 11. These signals are centered at 2982, 2989, 3068 and 3077 cm^{-1} (Table 3). [18] Several bands are observed in the fingerprint region NO_2 deformations and stretches coupled to C-H and N-N and C-N-C deformations between 1300 and 1000 cm^{-1} [19] The most important and strongest Raman peak are at 880 and 1222 cm^{-1} are attributed to the symmetric ring-breathing mode and the N-N bond stretch, respectively (figure 12). [20]

Table 3. Assignments of vibrational modes of RDX

Frequency	vibrational mode
370- 380	C-N-C deformation *a*
849 – 860	CH_2 rocking and C-N-C deformation *a*
870- 900	ring stretching *b*
1200-1350	N-N strectch and Symmetric NO_2
1520 – 1590	asymmetric NO_2 strectch
2980-3070	C-H stretching

a y b Indicates assignments from ref [18] and [20] respectively

5.8 **Mixture of RDX with Aspirin**

Remote Raman spectra of RDX, aspirin and their 50% mixture in the fingerprint region 150-1800 cm^{-1} at a distance of 7 m from the telescope are shown in Fig. 13**.** These samples were detected using 488 nm laser beam with 1W and the acquisition time was 10 seconds for recording the spectrum. In the laboratory made mixture, it is possible to differentiate the peaks at 880 and 1600 cm^{-1}, corresponding to the symmetric ring-breathing in RDX and the C=O stretching mode in aspirin.
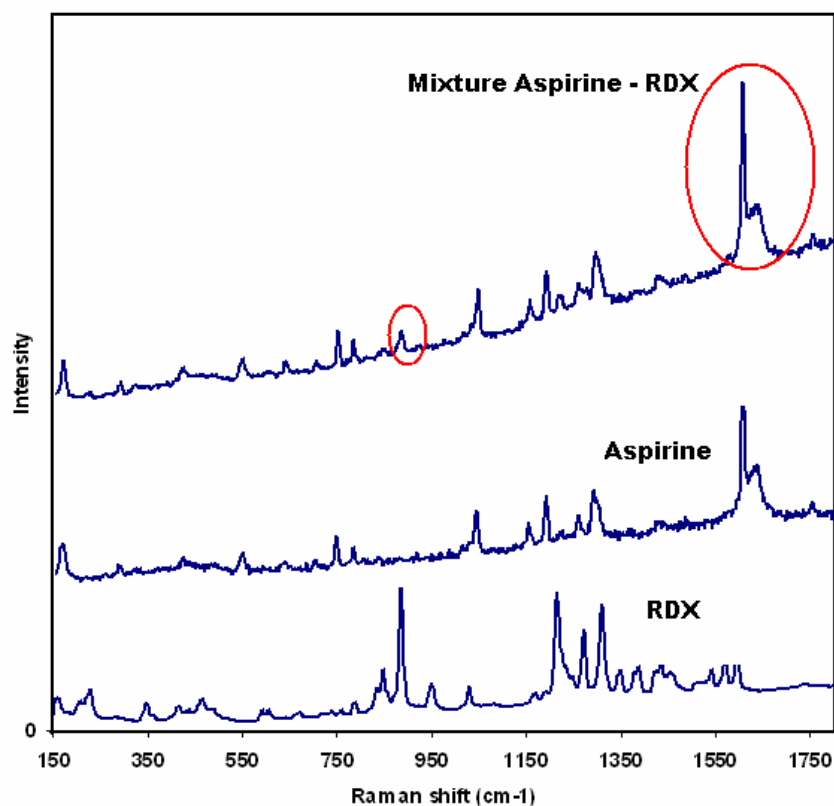

Figure 13 Remote Raman spectra of mixture of RDX and aspirin.

5.9 Quantification of explosives

In this study the laser power, the acquisition time and the mass of C4 were varied in order to find the conditions of minimum detectable Remote Raman signal as a function of these variables. For the study, the peak area for the prominent Raman signal of RDX 880 cm^{-1} was used. Figure 14 shows the obtained calibration graphs for C4. Calibration was performed by three repetitive measurements of mass ranging from 5 to 85 mg. Peak areas were integrated and graphed as a function of mass deposited on a stainless steel plate used for sample support. Error bars for each data point represent the calculated standard deviation derived from three repetitive measurements each. Each straight line represents the variation of Raman signal detected at a fixed integration time. Similar representations were obtained as laser power dependences as a function of mass at fixed integration times. These plots were put together as Detection Profiles: Power-Acquisition Time-Mass dependence. One such representation is shown in Fig. 15 for C4 for laser powers from 0.05 to 1W; acquisition time from 1 to 50 s and mass of 1 to 90 mg. All these data is presented in Table 4.
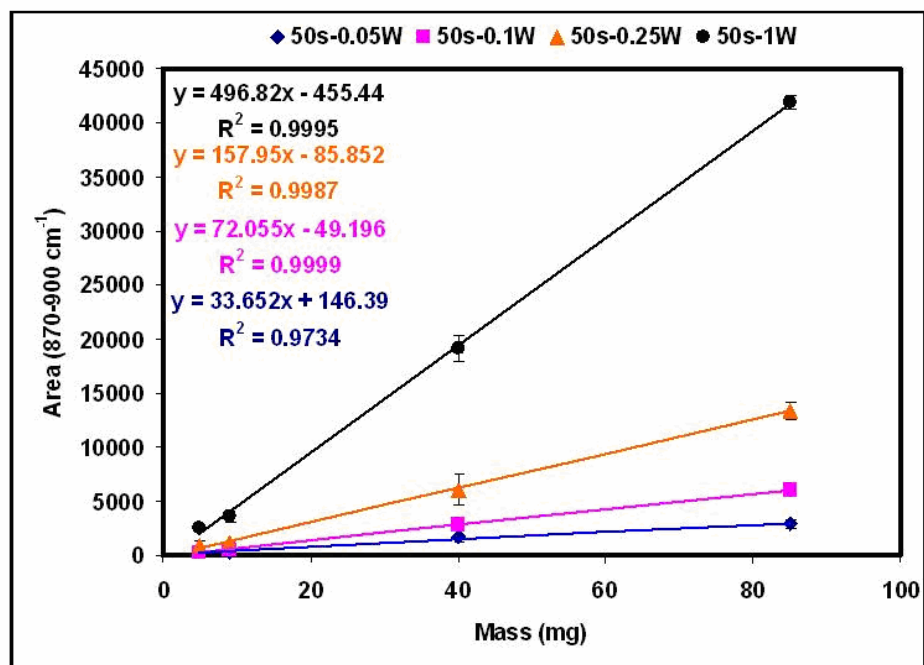
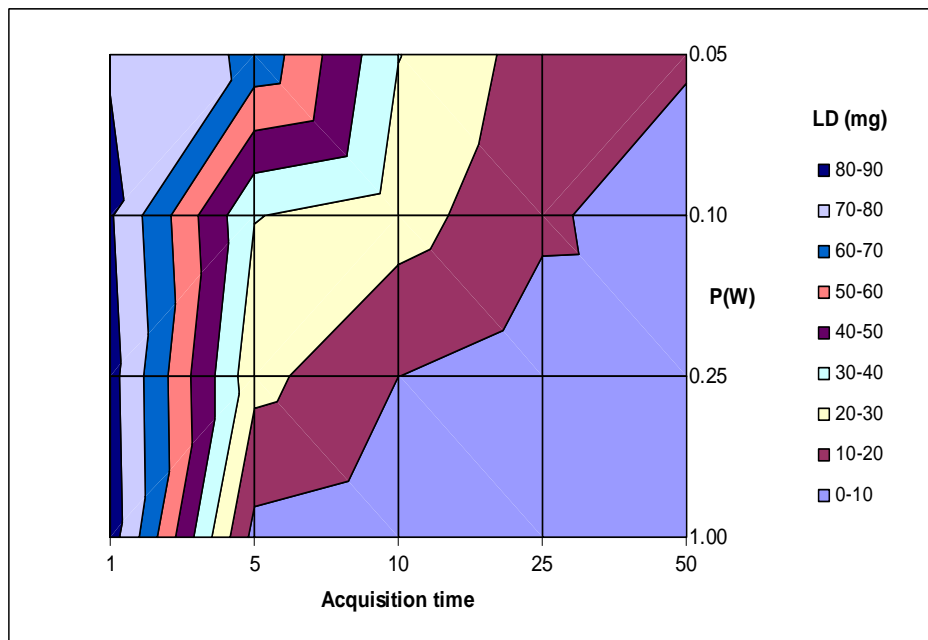**Figure 14 Calibration graphs for C4, varying power laser and acquisition time.**

Figure 15 Detection of C4 varying amount, power and integration time

Table 4. Detection limits of C4 at different conditions.

Power (W)	Acquisition time (s)	LD (mg)
0.05	1	80
0.1	1	81
0.25	1	84
1	1	85
0.05	5	68
0.1	5	30
0.25	5	23
1	5	7
0.05	10	30
0.1	10	24
0.25	10	10
1	10	3
0.05	25	15
0.1	25	12
0.25	25	5
1	25	3
0.05	50	12
0.1	50	3
0.25	50	4
1	50	2

Detection limits for each explosive have been calculated according to IUPAC by the 3σ

criteria (3 times standard deviation of the peak-to-peak noise related to the slope of the

linear regression function) and resulted in LODs below of 10 mg, These values represent a significant improvement from this work and other relevant spectroscopic approaches to explosive remote determination are summarized in Table 5.

Table 5. Detection limits were calculated for condition: P =1W, beam diameter 3.5 mm, acquisition time=10s, distance=7 m.

Explosive	LD (mg)
C4 (488nm)	3
2,4-DNT (514nm)	2
TNT (514nm)	2
RDX (488nm)	3
TATP (514 nm)	10
Semtex	ND

5.10   **Remote Raman spectra of Chemical Warfare Agents simulants CWAS**

The spectra of three Chemical Warfare Agents Simulants (CWAS) 2-CEES, 2-BAET and DMMP are shown in Figure 16. All spectra were collected at a distance of 7 m from the telescope. The samples were detected using 488 nm laser beam with 1W and the acquisition time was 10 seconds for recording the spectra.
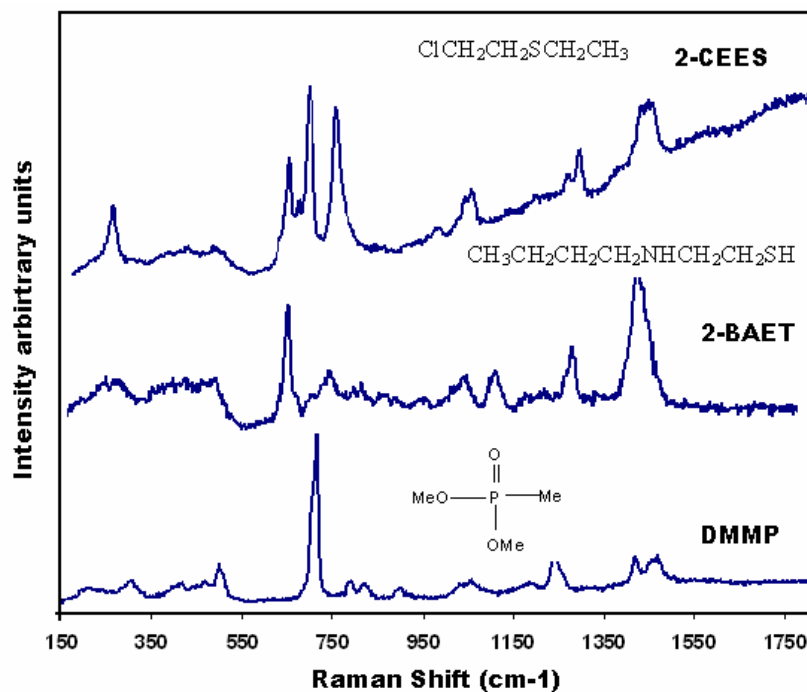
Figure 16 Remote Raman of Chemical Warfare Agents simulants.

The peak at 715 cm^{-1} for DMMP corresponds to a stretching mode involving the phosphorus atom and a much stronger line at around 700 correspond to C-Cl and 660 and 750 cm^{-1} C-S and C-S-C stretching modes of CEES, and the peaks around 660 and 1440 cm^{-1} can be assigned to C-S stretching and C-N stretching vibrations, respectively for 2-BAET simulant.

5.11   **Quantification of DMMP in water**

In order to carry out the quantification of DMMP in water solutions of the analyte ranging from 5 to 50% were prepared and analyzed using Remote Raman Spectroscopy.

For DMMP quantification, the peak area of the strongest Raman signal located about 715 cm^{-1} was used (Fig. 17).
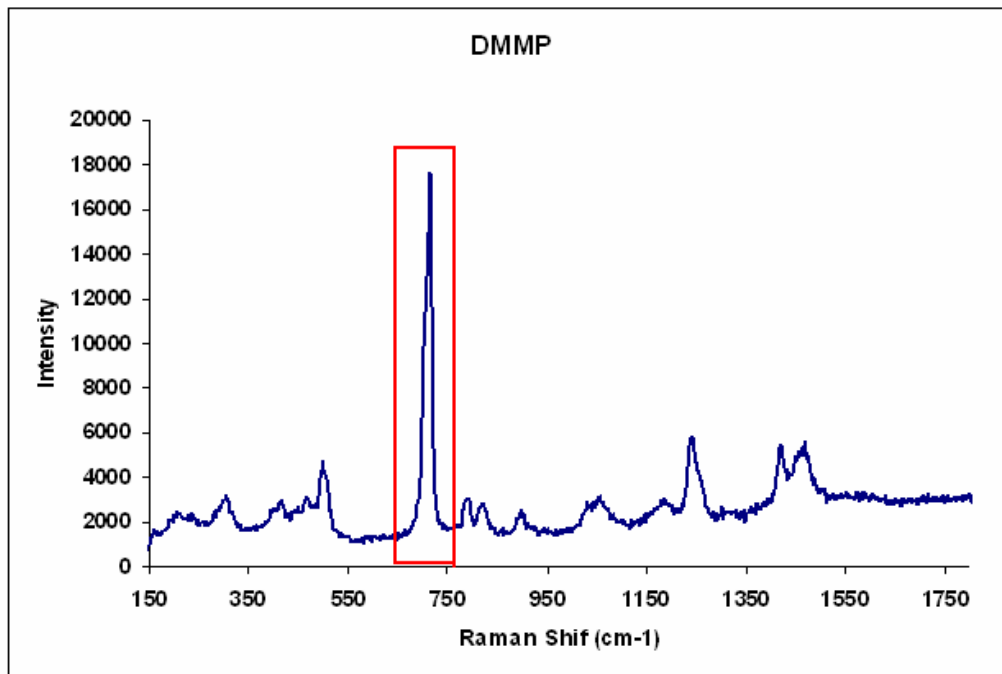

Figure 17 DMMP's area used to quantification in water.

Figure 18 shows the obtained calibration graphs for the investigated analytes in aqueous solution. Calibration was performed by three repetitive measurements of a concentration series ranging from 50% (v/v) to 1% ppm (v/v) for DMMP, using 850 mW power and integration time of 10 seconds. Error bars for each data point represent the calculated standard deviation derived from all repetitive measurements each. Detection limits for this analyte has been calculated according to IUPAC by the 3σ criteria (3 times standard deviation of the peak-to-peak noise related to the slope of the linear regression function) and resulted in LODs of 4 (%w/v).
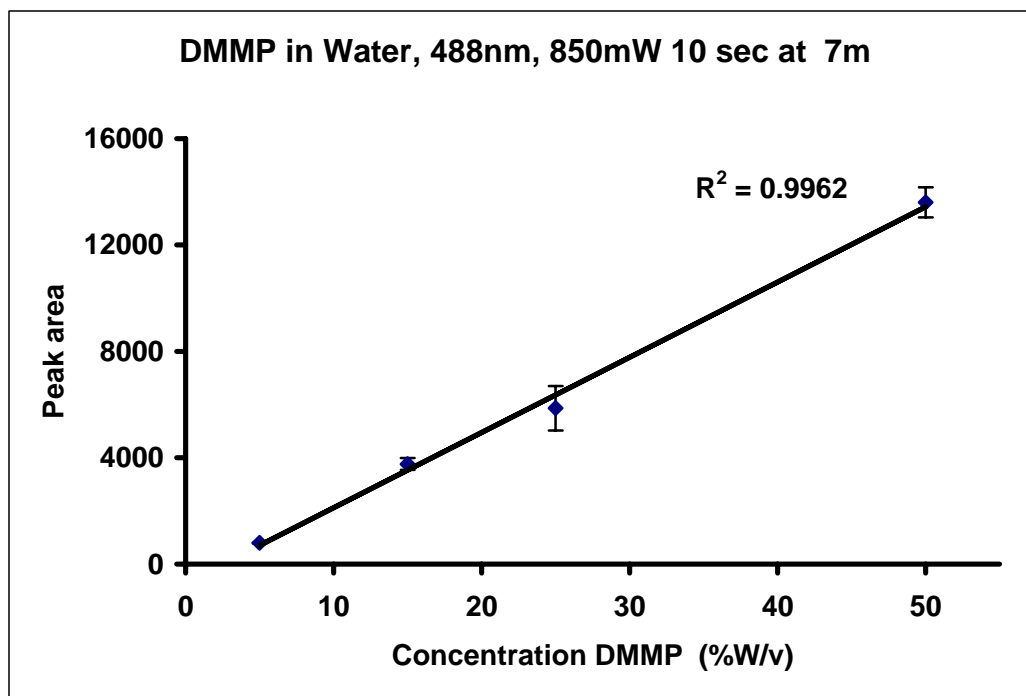
Figure 18 Calibration graphs for DMMP in water.

5.12 Remote Raman spectra of Toxic Industrial Compounds

Several compounds important in process development in petrochemical and other chemical industries are toxic, mutagenic or carcinogenic. Thus, it is vital to find different ways of monitoring these compounds. Standoff Raman systems offer new and easy alternatives to carry out this process remotely. Figures 19-21 illustrate the remote Raman spectra of some organic solvents which are constituent of hydrocarbons mainly found in gasoline. All these spectra were collected at a distance of 7 m from the telescope under lab condition with lights off. The samples were detected using 514 nm laser excitation at 1W (measured at head) and an acquisition time of 10 seconds.

The strong Raman band corresponding to symmetric stretching mode of the benzene ring at 992 cm^{-1} [22-23], in case of toluene and chlorobenzene the same band appears at 1003 cm^{-1}, another characteristic band in toluene is at 786 cm^{-1}, and the C-Cl stretching mode of chlorobenzene is clearly observed around 700 cm^{-1} in the Raman Shift spectra.
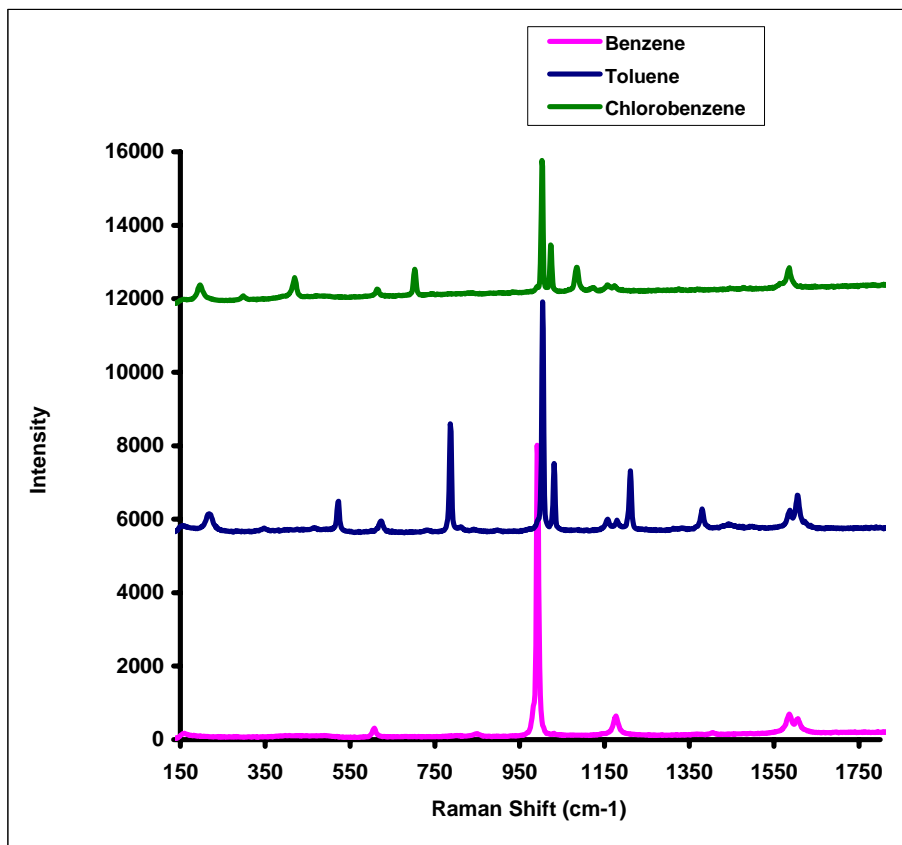

Figure 19 Raman spectra of aromatic compounds in fingerprint region.

Figure 20 contains Raman spectra of isomers of xylenes in the 150–1800 cm^{-1}, recorded at a distance of 7m from the telescope. The Raman bands in the wavenumber range 700–860 and 960–1080 cm^{-1} are often used for determination of these compounds in gasoline and environmental samples.[24-25] The *ortho, meta,* and *para*-xylene positional isomers have characteristic Raman bands at, 734, 726, and 828 cm^{-1}, respectively. The aromatic

ring stretch gives rise to a strong Raman band at 992 cm^{-1} in the spectrum of benzene, in the spectra of xylenes these aromatic ring stretching modes can be used as sensitive indicators of aromatic compounds in mixtures.
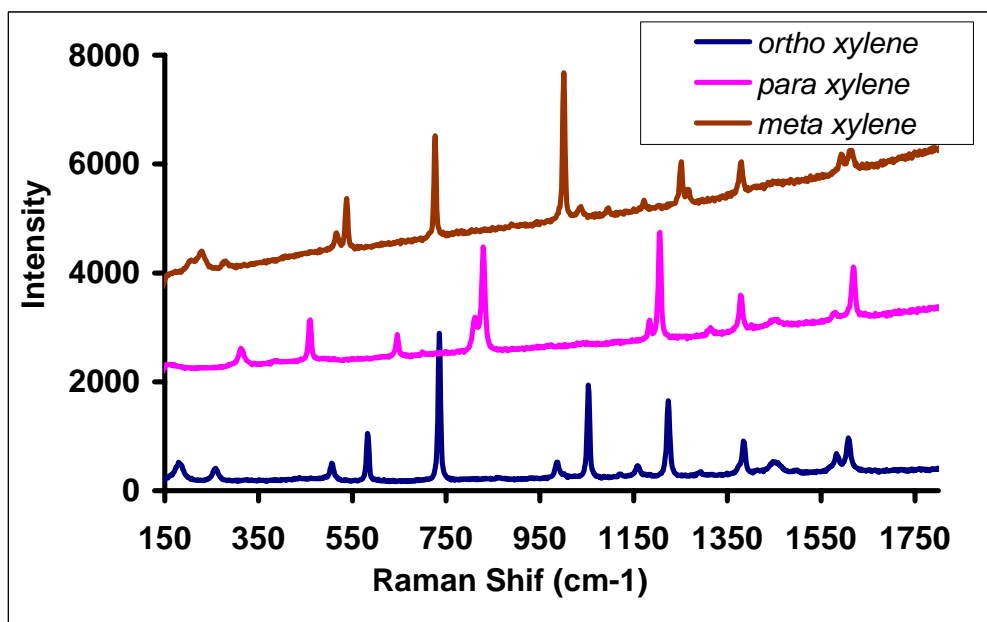

Figure 20 Raman spectra of isomers of xylenes in the 150–1800 cm^{-1}

Several organic solvents are widely used in the industry and also at lab scale, such as carbon disulfide, carbon tetrachloride and cyclohexane. All these compounds have particular characteristics mainly the cyclohexane, this one is used as one of the standards for calibrating Raman spectra. In this work, we also have measured the Raman spectra of these compounds contained into 5 mL clear glass vial in the 150–1800 cm^{-1} region at stand-off distance of 7 m (Fig. 21).

It possible to identify carbon disulfide by its very strong peak around at 655 cm^{-1} corresponding C-S symmetric stretching mode, the same for the carbon tetrachloride that has three mainly peaks. The most important band for CCl$_4$ appears at 461 cm^{-1}; this band

is attributed to C-Cl symmetric stretching modes. According to the literature, cyclohexane is characterized by four prominent bands in the 800-1650 cm^{-1} region: a very strong peak at 801 cm^{-1} due to the C–C breathing mode, the other weak peaks that appear at 1230, 1260 and 1445 cm^{-1} are due to C–C stretching modes.
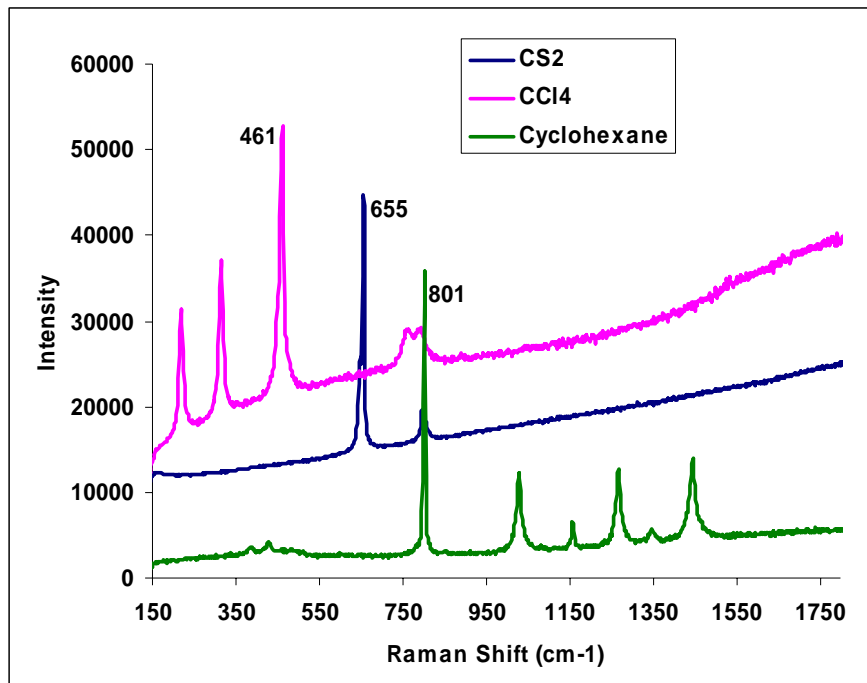

Figure 21 Raman spectra for carbon disulfide, carbon tetrachloride, and cyclohexane used in this work

6   CONCLUSION

A Standoff Raman system has been constructed by coupling a Raman Spectrometer with a reflective telescope by fiber optics employing 488 and 514 nm lasers as excitation lines. This prototype was tested in the detection of high explosives (HE): TNT, DNT, TATP, RDX and plastic explosive C4; chemical warfare agents simulants (CWAS): DMMP, 2-CEES and 2-TAEB and hazardous liquids.

The operational range of the Standoff system was tested to 7 m at laboratory scale, under dark conditions. Quantification of explosives was accomplished with detection limits below 10 mg. In addition, quantification of DMMP in water accomplished with a low limit of detection of 4%w/v.

The designed and tested remote Raman system allowed the detection organic solvents and mixtures of RDX and aspirin. It is important to mention that all chemical substances employed in this work were detected with a 514 nm excitation line except for C4 (RDX) which required 488 nm. Semtex, another plastic explosive of wide military application, could not be detected employing this system. The remote Raman system designed in this work will be useful for defense and security applications and monitoring environmental pollution, and for identifying unknown materials.

7 FUTURE WORK

Future work in this area can be basically focused to the detection of compounds previously studied at different distances and, particularly in volatile explosive in gas phases such as TATP and TNT, it is possible to contribute to the study of mixture of explosives implementing a Chemometrics analysis for quantifying analytes in more complex mixtures.

8   BIBLIOGRAPHY

1. Sun, Y.; and Ong, K. Y.; Detection Technologies for Chemical Warfare Agents and Toxic Vapors (CRC Press, Boca Raton, FL, **2005**).

2. Farquharson, S.; Gift, A.; Maksymiuk, P.; Inscore F. Surface-enhanced Raman spectra of VX and its hydrolysis products, *Appl. Spec*. **2005**, *59*, 654-659.

3. Smentkowski, V. S.; Hagans, P.; Yates, J. T. Study of the Catalytic Destruction of Dimethyl Methylphosphonate: Oxidation over Mo(ll0), *Phys. Chem*.**1988**, 92, 6351-6357.

4. Marrs, T. C.; Maynard, R. L.; Sidell, F. R. Chemical Warfare Agents: Toxicology and Treatment, (John Wiley & Sons Ltd., London, UK, **1996**).

5. Steinfeld, J.I.; Wormhoudt, *Annu. Rev. Phys. Chem*. **1998**, *49*, 203.

6. Hirschfeld, T. Range Independence of Signal in Variable FocusRemote Raman Spectrometry. *Appl. Opt*. **1974**, *13*, 1435.

7. Angel, S.M.; Kulp, T.J.; Vess, T.M. *Appl. Spec*. **1992**, *46*, 1085.

8. Wu, M.; Ray, M.; Fung, K.H.; Ruckman, M.W.; Harder, D.; Sedlacek III, A.J. Stand-off detection of chemicals by UV Raman spectroscopy. *Appl. Spectrosc.* **2000**, *54*, 800-806.

9. Sedlacek III, A.J.; Ray, M.D.; Higdon, N.S.; Richter, D.A. Short-range noncontact detection of surface contamination using Raman lidar *Proc. SPIE*. **2001**, *95,* 4577.

10. Sharma, S.K.; Angel, S.M.; Ghosh, M.; Hubble, H.W.; Lucey, P.G. A remote pulsed-laser Raman spectroscopy system for mineral analysis on planetary surfaces to 66 meters. *Appl. Spectrosc* **2002**, *56*, 699-705.

11. Thomson, G.; Batchelder, D. *Rev. Sci. Instrum.* **2002**, *73*, 4326.

12. Sharma, S.K.; Lucey, P.G.; Ghosh, M.; Hubble, H.W.; Horton, K.A. Stand-off Raman Spectroscopic Detection of Minerals on Planetary Surfaces. *Spectrochim. Acta A* **2003**, *59*, 2391-2407.

13. Sharma, S.K; Anupam, K.M; Bhavna S. Portable remote Raman system for monitoring hydrocarbon, gas hydrates and explosives in the environment *Spectrochimica Acta Part A: Molecular and Biomolecular Spectroscopy August* **2005***, 61*, 2404-2412.

14. Misra, A.; Sharma S. K.; Lucey, P. G. Remote Raman Spectroscopy detection of minerals and or organics under illuminated conditions from a distance of 10 m using a single 532 nm laser pulse. *Appl. Spectrosc.* **2006**, *60*, 223-228.

15. Carter, J. C.; Angel, S. M.; Lawrence-Snyder, M.; Scaffidi, J.; Whipple, R. E.; Reynolds, J. G. Standoff detection of high explosive materials at 50 meters in ambient light conditions using a small Raman instrument. *Appl. Spectrosc.* **2005**, *59*, 769–775.

16. Sharma, S.K.; Lucey, P.G.; Ghosh, M.; Hubble, H.W.; Horton, K.A. Stand-off Raman Spectroscopic Detection of Minerals on Planetary Surfaces,. *Spectrochim. Acta A* **2003**, *59*, 2391-2407.

17. Birke, R. L.; Lombardi, J. R.; Gale, in R. J. ed. Spectroelectrochemistry theory and practice, Plenun, New York, **1998** 263-328

18. Torres, P.; Mercado, L.; Cotte, I.; Hernandez, S. P.; Mina, N.; Santana, A., Chamberlain, R. T.; Lareau, R.; Castro, M. E. Vibrational Spectroscopy Study of β and α RDX Deposits. *J. Phys. Chem. B,* **2004**, *108*, 8799 -8805.

19. Rice, B. M.; Chabalowski, C. F. *Ab Initio* and Nonlocal Density Functional Study of 1,3,5-Trinitro-*s*-triazine (RDX) Conformers. *J. Phys Chem. A* **1997**, *101*, 8720-8726.

20. Lin-Vien, D.; Colthup, N. B.; Fateley, W. G.; Grasselli, J. G. *The Handbook of Infrared and Raman Characteristic Frequencies of Organic Molecules* Academic Press: San Diego, CA, **1991**.

21. Dubnikova, F.; Kosloff, R.; Almog, J.; Zeiri, Y.; Boese, R.; Itzhaky, H.; Alt, A.; Keinan, E. Decomposition of Triacetone Triperoxide Is an Entropic Explosion. *J. Am. Chem. Soc.*; **2005**, *127*, 1146-1159.

22. Karpowicz, R. J.; Brill, T. B. Comparison of the molecular structure of hexahydro-1,3,5-trinitro-s-triazine in the vapor, solution and solid phases. *J. Phys. Chem.* **1984**, *88*, 348-352.

23. Shimanouchi, T.; Tables of Molecular Vibrational Frequencies Consolidated, vol. 1, National Bureau of Standards, **1972**.

24. Sverdlov, L.M.; Kovner, M.A.; Krainov, E.P.; Vibrational Spectra of Polyatomic Molecules. Moscow: Nauka, **1970.**

25. Stellman, C.M.; Ewing, K.J.; Bucholtz, F.; Aggarwal, I.D.; *Sens. Actuators* B 53 **1998**,173.

26. Skinner, H.T.; Cooney, T.F.; Angel, S.M. *Appl. Spectrosc.* 1996, *50,* 836